Int. J. Electrochem. Sci., 11 **(2016)** 3050 - 3055

International Journal of
ELECTROCHEMICAL
SCIENCE
www.electrochemsci.org

Short Communication

Solvent dependent in situ growth of Ni_xS_y supported on nickel foam as electrocatalysts for oxygen evolution reaction

Yong-Ming Chai[1], *Xiao Shang* [1], *Guan-Qun Han*[1, 2], *Bin Dong*[1,2,*] *Wen-Hui Hu*[1], *Yan-Ru Liu*[1], *Xiao Li*[1], *Chen-Guang Liu*[1,*]

[1] State Key Laboratory of Heavy Oil Processing, China University of Petroleum (East China), Qingdao 266580, PR China
[2] College of Science, China University of Petroleum (East China), Qingdao 266580, PR China
[*]E-mail: dongbin@upc.edu.cn, cgliu.upc.edu.cn@gmail.com

Received: 23 December 2015 / *Accepted:* 8 February 2016 / *Published:* 1 March 2016

In situ growth of Ni_xS_y on nickel foam (Ni_xS_y/NF) has been investigated by hydrothermal or solvothermal process in water, ethanol and their mixture. XRD shows that the obtained Ni_xS_y is consisted of Ni_3S_2 and NiS in the three solvents. Ni_xS_y synthesized in ethanol has weaker peak intensities and more NiS planes, implying lower crystallinity and different electrocatalytic properties from the other two smaples. SEM images confirm regular morphology transform of Ni_xS_y/NF affected by different solvents. Nanorods and polyhedron structure of Ni_xS_y can be observed in water and ethanol, respectively. For mixture solvents, obvious transition morphology including some nanorods and polyhedron structures can be observed. Electrochemical measurements for oxygen evolution reaction (OER) reveal that Ni_xS_y/NF synthesized in ethanol has the earliest onset potential (1.24 V vs. RHE) and the largest current density, which may be derived from different crystal structure and morphology of Ni_xS_y. Therefore, the solvent dependent activity may provide a new way to prepare excellent electrocatalysts for OER.

Keywords: crystal structure; solvent effect; microstructure; in situ growth; Ni_xS_y/NF

1. INTRODUCTION

Water splitting has been highlighted as environmental friendly methodology of producing hydrogen to address energy crisis and pollution caused by fossil fuels [1-3]. Great efforts have been devoted on selecting economical and efficient electrocatalysts to accelerate OER process to replace highly active but expensive ones such as IrO_2 or RuO_2 [4, 5].Transition metal sulfides and oxides have been broadly investigated because of good performances for OER and abundance in nature [6-8].

Steven L. Suib's group have reported that electrocatalytic performances of MnO_2 are strongly determined by crystalline structures [9]. Another report proved construction effects on NiS and Ni_3S_2 for different hydrogen evolution reaction (HER) activities [10]. Based on the above, it can be predicted that crystal structure and morphology of electrocatalysts exert great impact on catalytic activity. Moreover, excellent conductivity and robust structure are required to improve efficiency of active sites and stability for ideal electrocatalysts [11]. Owing to large surface area of three-dimensional porous structure of nickel foam (NF), active sites can be increased with better dispersion of active components. In addition, excellent conductivity of NF help promoting current densities and stabilities [12]. Therefore, in situ growth of electrocatalysts based on NF may be a promising choice for obtaining remarkably electrocatalytic activity.

Herein, we prepared in situ growth Ni_xS_y supported on NF through hydrothermal or solvothermal process, controlling structure and morphology with ethanol, water and their mixture as solvents, respectively. XRD illustrate that as-prepared Ni_xS_y are all composed of Ni_3S_2 and NiS. The crystallinity and ratio of Ni_3S_2 and NiS have been greatly affected by different solvent. SEM images confirmed different morphologies including nanorods, polyhedron and their mixture structures. Electrochemical measurements show that Ni_xS_y synthesized in ethanol has better electrocatalytic properties for OER.

2. EXPERIMENTAL SECTION

2.1 Preparation of Ni_xS_y/NF

NFs (Shenzhen Poxon Machinery Technology Co., Ltd.) with 1×2 cm^2 were cleaned in a 0.5 M H_2SO_4 by ultrasonication for 0.5 h to remove oxides, followed by ethanol and deionized water for 0.5 h. Next, 2 g of thiourea (CN_2H_4S) were added to 60 ml absolute ethanol, deionized water and water-ethanol solution with volume ratio of 1:1 (all solvents were purged by nitrogen for 30 min in advance to eliminate oxygen) to be blended uniformly. Then they were transferred into Teflon stainless steel autoclaves, added by NFs separately. They were heated at 140°C for 12 h, then cooled down to room temperature. Finally, samples were washed with water several times, dried in vacuum at 60°C for 8 h. Three samples were denoted as S-1(in water), S-2 (in half ethanol and half water) and S-3 (in ethanol), respectively.

2.2 Physical characterization

X-ray powder diffraction (XRD, X'Pert PRO MPD, Cu KR) was employed to investigate crystalline structure of samples, with 2θ data from 5˚ to 76˚. Scan electron microscopy (SEM, Hitachi, S-4800) was utilized to study detailed morphologies.

2.3 Electrochemical tests

Electrochemical tests were performed on an electrochemical work station (Gamry Reference 600 Instruments, USA) with a three-electrode system (three samples as working electrodes, platinum gauze as counter electrode and a saturated calomel electrode (SCE) as the reference). Linear sweep voltammetry (LSV) measurements were conducted with scan rate was 5 mV s^{-1} in 1 M KOH solution (purified by oxygen for 0.5 h beforehand). Electrochemical impedance spectroscopy (EIS) measurements were undertaken at 0.2 V (vs. SCE) with frequency from 100 KHz to 0.01Hz with an AC voltage of 5 mV. Cyclic voltammogram (CV) was performed to test stability of S-1 from 0.2 V to 0.4V (vs. SCE) in 500 cycles with scan rate of 100 mV s^{-1}.

3. RESULTS AND DISCUSSION

Figure 1 shows XRD patterns of all samples, containing Ni_3S_2 phase and NiS phase. Additionally, (111) and (200) planes can be assigned to Ni (JCPDS no. 65-2865) from NF. As for S-1 and S-2, only (101), (003), (211) planes of Ni_3S_2 and (300), (321) facets of NiS can be found, and corresponding peaks are more intense than that of S-3. Moreover, (312) plane of NiS appears on S-1 and S-2. In S-3, Ni_3S_2 involves (101), (110), (003), (211) planes (JCPDS no. 44-1418), and NiS contains (300), (021), (211), (131) and (321) facets (JCPDS no. 21-0041). Significant changes above suggest that different solvents influence crystallinity and phases during Ni_xS_y growth. Specifically, Ni_xS_y is amorphous in S-3, and has more NiS facets than the others. It can be speculated that ethanol promotes more planes of NiS and lower the crystallinity, whereas water and their mixture do not. This implies that S-3 may have more active sites for OER.

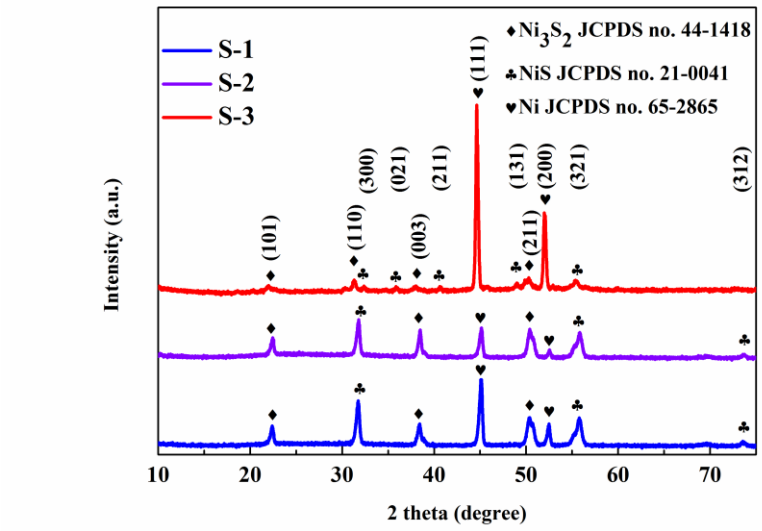

Figure 1. XRD patterns of S-1 (ethanol), S-2 (water) and S-3 (half ethanol and half water).

SEM images of three samples are shown in Figure 2. In Figure 2a, S-1 has an integral film of Ni_xS_y covering on NF. Under higher magnification (Figure 2b and 2c), Ni_xS_y film is mainly composed of nanorods with diameter of 200 nm and the length of about 1 μm, which should be Ni_2S_3 crystal phase [13]. However, the NiS phase detected in XRD (Figure 1) can hardly be observed through SEM, which may be covered by large amount of Ni_3S_2. SEM images of S-2 are shown in Figure 2d, 2e and 2f. Owing to mixture solvent of water and ethanol, Ni_xS_y film of S-2 is different from that of S-1 (Figure 2d).

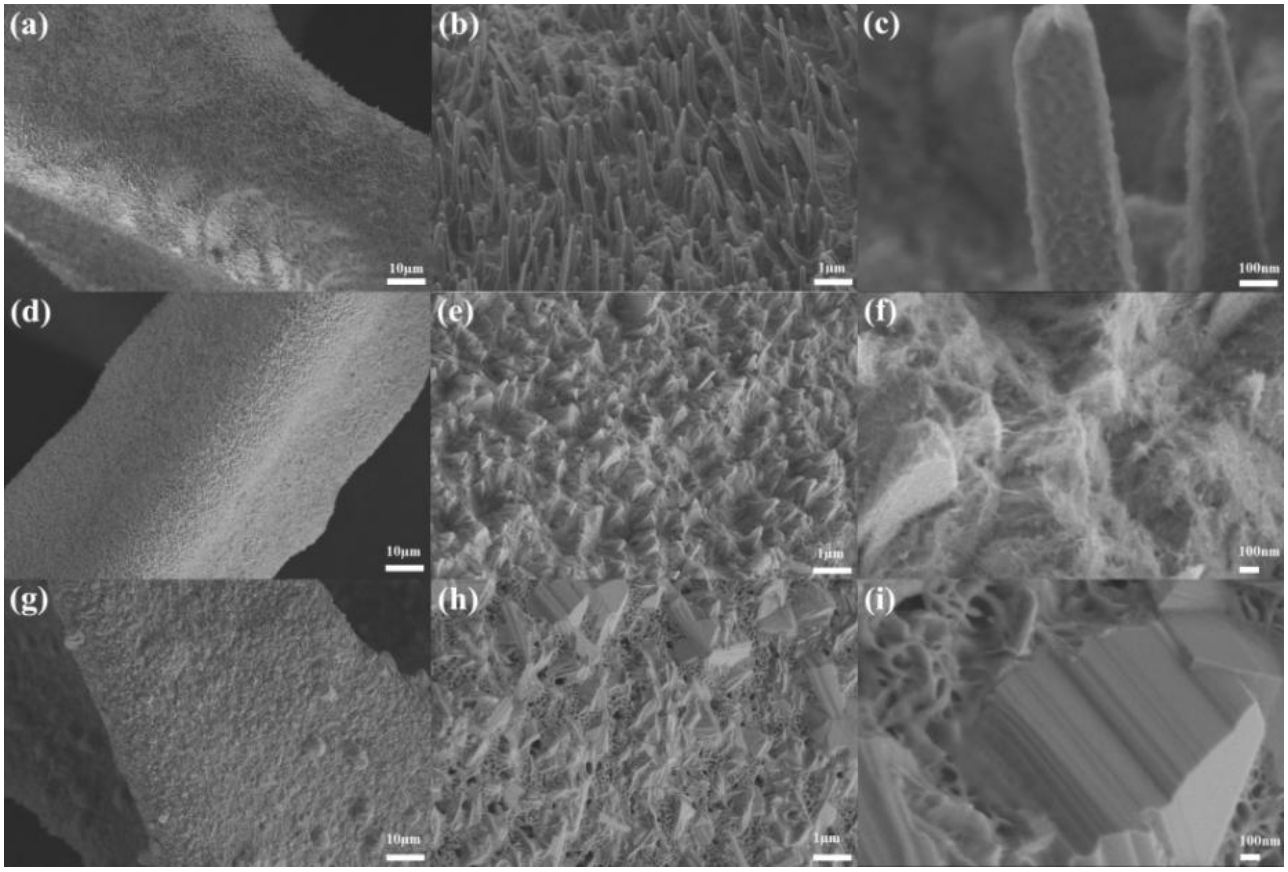

Figure 2. SEM images of S-1 (a-c), S-2 (d-f) and S-3 (g-i).

Figure 2e clearly shows the great decrease of the length of nanorods, suggesting that mixed solvent brings impact on morphology of Ni_3S_2. Moreover, it can be clearly seen from Figure 2f that nanorods have transformed to polyhedral structures with smaller size. With the increasing of ethanol, more changes of morphology of Ni_xS_y can be observed. For pure ethanol as solvent, Figure 2g shows distinct differences of Ni_xS_y film of S-3 compared with S-1 and S-2. Higher magnification of SEM (Figure 2h) displays many polyhedron structures dispersing on Ni_xS_y film of S-3, with disappearance of nanorod structures. In Figure 2i, polyhedron structures are accumulated by flake-like crystals of Ni_xS_y [14]. Although most of nanorods structures of Ni_3S_2 disappear, the porous and interconnected part on the Ni_xS_y film of S-3 observed may be derived from amorphous phases of Ni_3S_2 and NiS [15, 16], consistent with related XRD results.

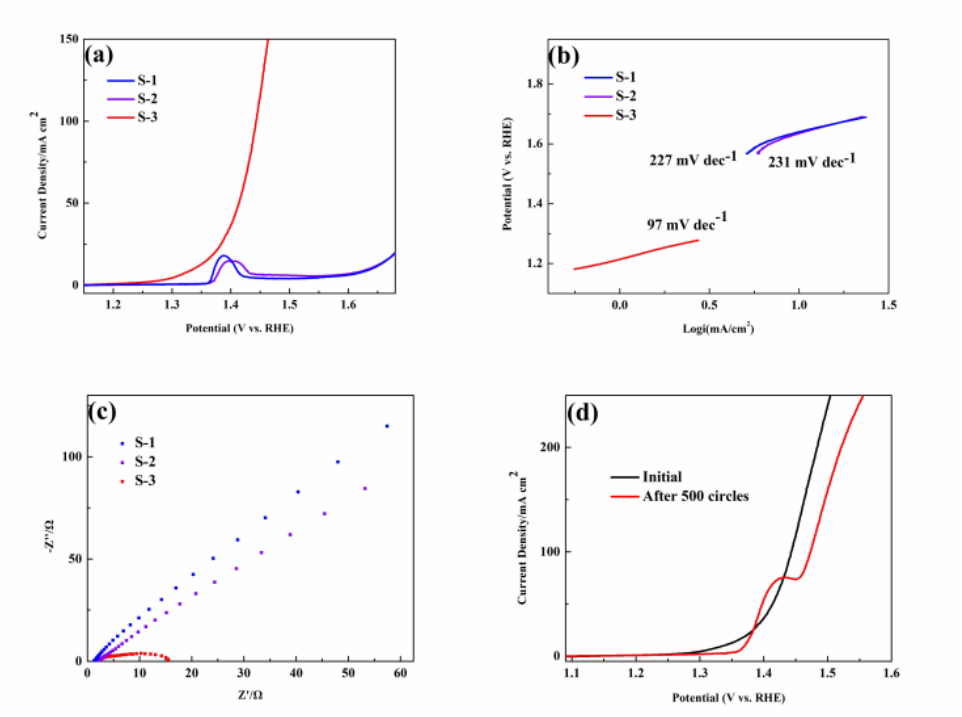

Figure 3. Electrocatalytic properties for OER of S-1, S-2, and S-3. (a) LSV; (b) Tafel Plots; (c) EIS; (d) Stability.

Figure 3 shows electrocatalytic performances of three samples for OER. Figure 3a displays evident differences of LSV curves of the three samples. Apparently, S-3 has an earlier onset potential (1.24 V vs. RHE) than that of S-1 and S-2 (1.55 V vs. RHE), with much higher current density after 1.25 V (vs. RHE). It can be speculated that more NiS facets of in S-3 may expose more activity sites for OER, corresponding with previous analysis of XRD and SEM. The oxidation peaks at 1.395 V (vs. RHE) of S-1 and S-2 may be due to electro-oxidized metal Ni on NF [17]. Tafel plots based on Figure 3a are shown in Figure 3b. Tafel slope (97 mV dec^{-1}) of S-3 is much smaller than that of S-1 (227 mV dec^{-1}) and S-2 (231 mV dec^{-1}), implying enhanced OER properties of S-3. Figure 3c displays EIS curves of all samples. S-3 exhibits the smallest impedance value compared with the others, revealing smaller charge-transport impedances. The enhanced conductivity of S-3 is favorable for electrocatalytic activity for OER. In Figure 3d, stability test after 500 cycles illustrates that S-3 has good stability. However, an oxidation peak at 1.41 V (vs. RHE) appears with the long period, which may account for Ni (II) being oxidized to Ni (III) under base media [18].

4. CONLUSIONS

A facile ethanol solvothermal method based on NF has been utilized to prepare in situ growth Ni_xS_y/NF with excellent electrocatalytic activity for OER. XRD and SEM demonstrate that ethanol alters crystal structures and morphologies of Ni_xS_y including more NiS phase. Electrochemical measurements indicate that Ni_xS_y/NF synthesized in ethanol have superior OER properties than that of

water or mixture solution, probably due to increased active sites on NiS. Therefore, selecting a specific solvent may provide a new strategy for controlling desirable crystal structure and morphology of electrocatalysts with high performances for OER.

ACKNOWLEDGEMENTS
This work is financially supported by the National Natural Science Foundation of China (U1162203 and 21106185) and the Fundamental Research Funds for the Central Universities (15CX05031A).

References

1. W.-H. Hu, R. Yu, G.-Q. Han, Y.-R. Liu, B. Dong, Y.-M. Chai, Y.-Q. Liu and C.-G. Liu, *Mater. Lett.*, 161 (2015) 120.
2. X. Chia, A. Ambrosi, Z. Sofer, J. Luxa and M. Pumera, *ACS nano*., 9 (2015) 5164.
3. M. La, Y. Feng, C. Chen, C. Yang and S. Li, *Int. J. Electrochem. Sci*., 10 (2015) 1563.
4. T. Reier, M. Oezaslan and P. Strasser, *ACS Catal.*, 2 (2012) 1765.
5. R. Valdez, D. B. Grotjahn, D. K. Smith, J. M. Quintana and A. Olivas, *Int. J. Electrochem. Sci*., 10 (2015) 909.
6. W. Z. Teo, A. Ambrosi and M. Pumera, *Electrochem. Commun*., 28 (2013) 51.
7. G. An, L. Chenguang, Y. Hou, X. Zhang and Y. Liu, *Mater. Lett*., 62 (2008) 2643.
8. W. Tang, Y. Deng, W. Li, S. Li, X. Wu and Y. Chen, *Catal. Commun*., 72 (2015) 165.
9. Y. Meng, W. Song, H. Huang, Z. Ren, S. Y. Chen and S. L. Suib, *J. Am. Chem. Soc.*, 136 (2014) 11452.
10. D. Y. Chung, J. W. Han, D. H. Lim, J. H. Jo, S. J. Yoo, H. Lee and Y. E. Sung, *Nanoscale.*, 7 (2015) 5157.
11. Y. Wang, T. Zhou, K. Jiang, P. Da, Z. Peng, J. Tang, B. Kong, W.-B. Cai, Z. Yang and G. Zheng, *Adv. Eng, Mater*., 4 (2014) 1400696.
12. W. Zhou, X.-J. Wu, X. Cao, X. Huang, C. Tan, J. Tian, H. Liu, J. Wang and H. Zhang, *Energy Environ. Sci.*, 6 (2013) 2921.
13. W. Zhou, X. Cao, Z. Zeng, W. Shi, Y. Zhu, Q. Yan, H. Liu, J. Wang and H. Zhang, *Energy Environ. Sci.*, 6 (2013) 2216.
14. W. Cui, C. Ge, Z. Xing, A. M. Asiri and X. Sun, *Electrochim. Acta*., 137 (2014) 504.
15. L. Yu, B. Yang, Q. Liu, J. Liu, X. Wang, D. Song, J. Wang and X. Jing, *J. Electroanal. Chem*., 739 (2015) 156.
16. L. L. Feng, G. Yu, Y. Wu, G. D. Li, H. Li, Y. Sun, T. Asefa, W. Chen and X. Zou, *J. Am. Chem. Soc*., 137 (2015) 14023.
17. G.-Q. Han, Y.-R. Liu, W.-H. Hu, B. Dong, X. Li, X. Shang, Y.-M. Chai, Y.-Q. Liu and C.-G. Liu, *Appl. Surf. Sci*., 359 (2015) 172.
18. C. Sun, M. Ma, J. Yang, Y. Zhang, P. Chen, W. Huang and X. Dong, *Sci Rep*., 4 (2014) 7054.